Physica Medica 62 (2019) 105–110

Contents lists available at ScienceDirect

Physica Medica

journal homepage: www.elsevier.com/locate/ejmp

Original paper

Monte Carlo simulations of different CT X-ray energy spectra within CTDI phantom and the influence of its changes on radiochromic film measurements

Nada Tomic*, Pavlos Papaconstadopoulos, Hamed Bekerat, Golub Antunovic, Saad Aldelaijan, Jan Seuntjens, Slobodan Devic

Department of Radiation Oncology, Jewish General Hospital, Montréal, Québec, Canada
Medical Physics Unit, McGill University, Montréal, Québec, Canada

ARTICLE INFO

Keywords:
CTDI measurement
Radio chromic film

ABSTRACT

Purpose: In this work we use Monte Carlo simulations to investigate change in Computed tomography (CT) X-ray energy spectra between exposures in air and within CT dose index (CTDI) phantom. While the results of these simulations will be relevant when measuring CTDI with any dosimeter, we apply the appropriate beam quality change correction for CTDI measurements using XR-QA2 model GafChromic™ film.

Methods: Dose profiles were measured with film strips, sandwiched between acrylic rods cut in half, placed within CTDI phantoms and scanned before and after irradiation with document scanner in reflective mode. Reference dosimetry system was calibrated in terms of air kerma in air, which was converted into absorbed dose using ratio of mass-energy absorption coefficients water-to-air for a given beam quality, following the AAPM TG-61 protocol.

Results: Beam qualities for all film positions within CTDI phantom show beam softening for HVLs above 6 mm Al and beam hardening for HVLs bellow 6 mm Al. Calculated CTDI values using HVL in air for all CTDI positions, and those calculated using the appropriate calibration curves based on beam quality correction show for Head CTDI phantom differences ranging from 0.3% to 2.1% and for Body CTDI phantom from 2.5% to 5.7%.

Conclusions: We describe method for CTDI measurements using radiochromic film dosimetry protocol corrected by the beam quality change within the phantom. Our results show differences in CTDI measurements of up to 5.7% when compared to using film calibration curves for beam quality in air.

1. Introduction

Radiation output assessment in computed tomography (CT) is currently performed using the concept of CT dose index (CTDI) [1,2]. The measurement of the radiation index ($CTDI_{100}$) are performed with 100 mm long ion chamber to include scattering tails of axial scan and within specifically designed cylindrical CT dosimetry phantoms made of polymethyl methacrylate, 15 cm long and 16 cm in diameter (Head CTDI phantom) or 32 cm in diameter (Body CTDI phantom). Both phantoms have five 1 cm diameter holes with the purpose to place the dosimeter. The measured $CTDI_{100}$ is expressed as an integral of dose profile along the longitudinal direction. The CTDI concept consists also of calculating weighted CTDI ($CTDI_w$), which takes into account CTDI variations with depth. The final calculated CTDI parameter, the volumetric CTDI ($CTDI_{vol}$) takes into account the specific imaging protocol, the helical pitch or axial scan spacing for scans acquired by multi-slice CT scanners.

With the introduction of larger multi-detector arrays and by employing wider CT beams the concept of CTDI came under scrutiny as it was apparent that CTDI chambers were not recording the full scattering signal generated by the CT scans. The AAPM Task Group 111 [3] has proposed a new dosimetry index, the equilibrium dose (D_{eq}) measured by using small volume ionization chamber positioned at the center of an extended cylindrical phantom. On the other side, all manufacturers still provide the $CTDI_{vol}$ and dose-length product (DLP) for all CT scanning protocols on their scanner console as a mandatory requirement.

While the most commonly used dosimeter is the 100 mm long sensitive volume CTDI ionization chamber, a number of other radiation detectors have been investigated for this task. Although the semiconductor detectors (usually diodes) provide direct signal readout like

* Corresponding author at: Jewish General Hospital, 3755 Chemin de la Côte-Sainte-Catherine, Montréal, Québec H3T 1E2, Canada.
E-mail address: nada.tomic@mcgill.ca (N. Tomic).

https://doi.org/10.1016/j.ejmp.2019.04.015
Received 1 March 2019; Received in revised form 15 April 2019; Accepted 17 April 2019
Available online 11 May 2019

ionization chambers, they suffer from the significant energy dependent response and their response is observed to change with time, which requires frequent re-calibrations [4]. On the other hand, termo-luminescent detectors (TLDs) and optically stimulated luminescence detectors (OSL) not only require post-processing after the irradiation, but they also suffer from the significant energy dependent response [5,6]. The use of XR-QA2 model GafChromic™ film was suggested for the CTDI measurements and reported in the literature [7,8], having several advantages. One is that the film provides the information about the dose profile instead of point dose information. The second one is that only one scan is needed for CTDI measurement (five film strips placed at different positions within the phantom are simultaneously irradiated within the modified CTDI phantom). Due to such experimental setup, there is no stem and/or cable effect on measured signal. However, as in the case of the above-mentioned solid detectors, the XR-QA2 model GafChromic™ film also exhibits a significant change in its dose response with the change of the beam quality used [9,10].

For the purpose of CTDI measurements, any dosimeter used (as mentioned above) is calibrated in the air. Since the actual measurements are performed in phantom, the change of the beam quality in phantom at the point of measurement due to either beam hardening effect or scattering was reported [11]. The purpose of this work is to use Monte Carlo simulations to investigate and quantify the change in CT X-ray energy spectra between exposures in the air (assumed to be known for a given beam quality) and within CTDI phantom. While the results of this study will be relevant when measuring CTDI with any of the dosimeters mentioned so far (including even ion chambers that may have a small energy dependent response) we will use them to apply the appropriate beam quality change correction for CTDI measurements using XR-QA2 model GafChromic™ film.

2. Materials and Methods

2.1. Monte Carlo simulations of beam qualities

Monte Carlo calculations of energy spectra changes in a CTDI phantom were performed using the EGSnrc/cavity code (Fig. 1). To cover beam qualities used in modern CT scanners, the input spectra were generated by the SpekCalc software [12] at nominal energies of 100, 120, and 140 kVp with additional filtration and corresponding HVLs given in Table 1. Basic geometry parameters used in this work are source-to-isocenter distance of 60.6 cm, and collimator settings of 20 mm × 497 mm and 40 mm × 497 mm.

Photon spectra were captured at the center of each of the five holes within the CTDI phantom: top, bottom, left, right and center holes. Every photon passing a 1 cm diameter disk within CTDI phantom hole was captured. Monte Carlo simulations were carried on using the XCOM cross-section data with ECUT = 1 keV. Rayleigh scattering was turned on and Bremsstrahlung cross sections were taken from NIST database. We used Penelope electron impact ionization and no variance reduction techniques. To simulate spectra within CTDI phantom in the course of a CT scan, we rotated collimated source with a step of 1 degree from 0 to 360 degrees.

We also used NRC developed code for calculation of spectra metrics (HVL1, HVL2, E_{eff}, E_{av}) with a statistical accuracy of 0.2%. With XCOM cross-section. Entrance spectra metrics were re-calculated for consistency.

2.2. Radiochromic film based CTDI measurements

We used standard cylindrical CT dosimetry phantoms made of polymethyl methacrylate (PMMA), 15 cm long and 16 cm in diameter (Head CTDI phantom) or 32 cm in diameter (Body CTDI phantom), which were used with rods slightly modified to accommodate measuring pieces of XR-QA2 GafChromic™ film. Film pieces (15 cm × 1 cm in size) were sandwiched between acrylic rods cut in half and placed within CTDI Head and Body phantoms (Fig. 2). Unlike during the standard CTDI measurement procedure, whereby 5 different scans have to be performed between which 10 cm long CTDI ion-chamber has to be

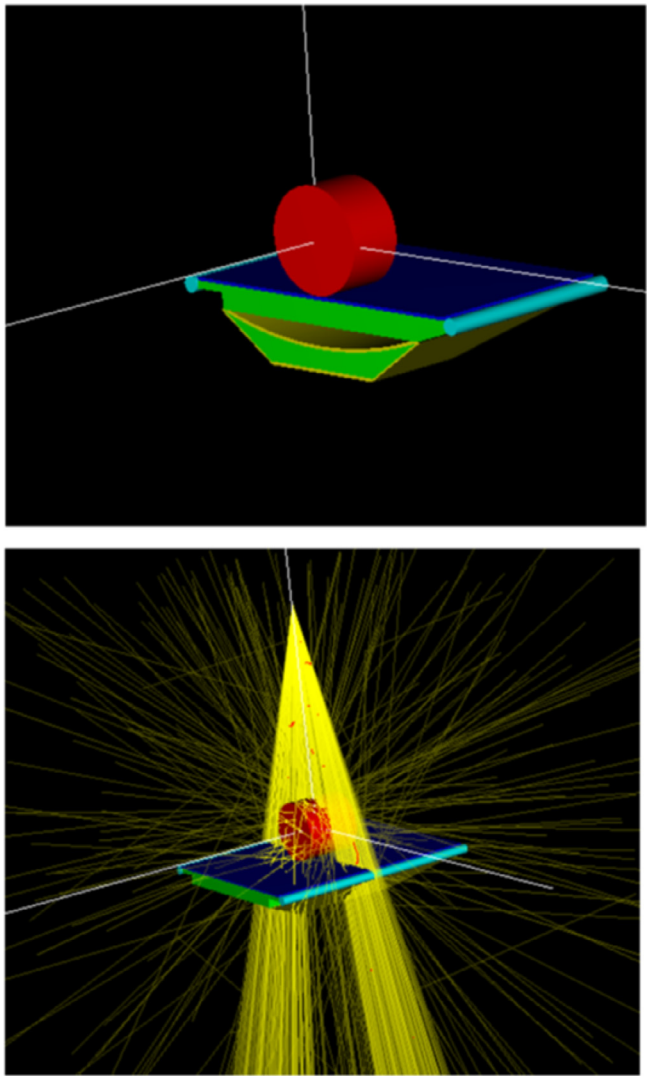

Fig. 1. Geometry used for Monte Carlo simulations of beam quality change within CTDI phantom.

Table 1
HVLs of the input spectra calculated for three kVp settings (100, 120, 120 kVp) and five additional filtrations (2, 4, 6, 8, 10 mm Al) at the center of the CT scanner in the air.

kVp	Filtration [mm Al]	HVL @ center [mm Al]
100	2	3.01
	4	4.35
	6	5.34
	8	6.06
	10	6.66
120	2	3.77
	4	5.29
	6	6.34
	8	7.12
	10	7.71
140	2	4.61
	4	6.20
	6	7.25
	8	8.00
	10	8.63

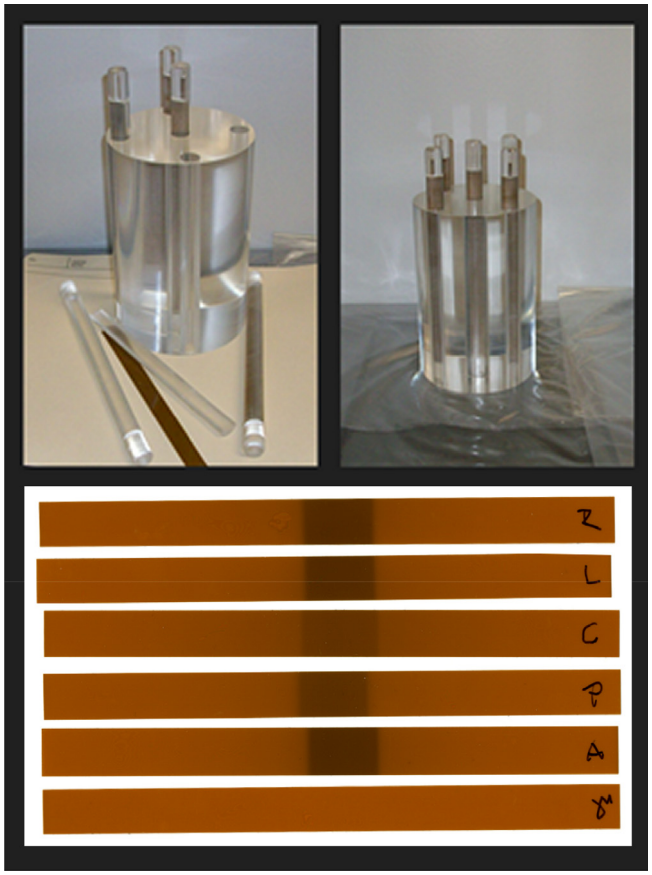

Fig. 2. Modified CTDI phantom to accommodate radiochromic film strips.

relocated from one hole to the other, in our measurement setup all five film pieces are irradiated at the same time. Another advantage of using film for CTDI measurement is that there is no stem (and/or cable) effect on the measured signal.

2.3. Calibration of the radiochromic film based reference dosimetry system

Response of the reference radiochromic film dosimetry system based on XR-QA2 GafChromic™ film model was calibrated in terms of air kerma in air. A General Electric Lightspeed LS 16 radiotherapy CT simulator was used for this purpose. Beam quality specifiers (half value layers (HVLs), and the device outputs (air kerma in air (cGy/mAs),) for each beam quality were obtained following the AAPM TG-61 protocol [13]. National Research Council of Canada (NRCC) calibrated Farmer type thimble chamber NE model 2577C and a Keithley model 6517A electrometer were used for the output measurements.

Pieces of GafChromic™ XR-QA2® film (2.5 cm × 5 cm in size) were irradiated in air at known air kerma values with the x-ray tube of the CT scanner in static mode. Film response in terms of reflectance change (relative change of pixel values) of the films prior and after irradiation (ΔR) was determined using an in-house routine made in MatLab, using the TIF images of the films acquired by an Epson Expression 10,000XL flatbed document scanner in reflection scanning mode. Pixel values were read after applying the 'wienner2' filter to extracted 16-bit deep red channel images obtained with 127 dpi (0.2 mm/pixel) scanning resolution. Reflectance change was calculated as a difference between reflectance of the unexposed film piece ($PV_{unexp}/2^{16}$) and the same film piece after exposure ($PV_{exp}/2^{16}$), where the PV_{unexp} and PV_{exp} represent averaged pixel values taken over 10 pixel by 10 pixel ROI (2 mm × 2 mm). More details about calculation of XR-QA2 film model response can be found in Reference [14]. Calibration curves are presented in Fig. 3 for beam qualities in the range from 4.03 to 8.25 mm Al,

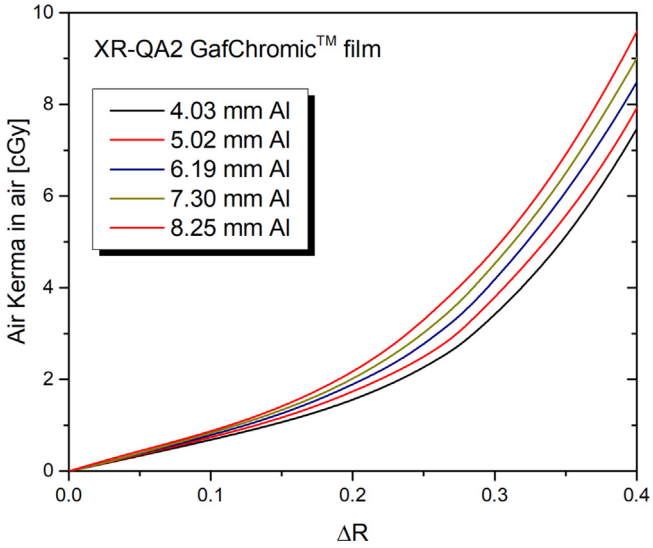

Fig. 3. Calibration curves for XR-QA2 GafChromic™ film based reference dosimetry system for different beam qualities with air kerma in air as a function of relative reflectance change of films prior and after the irradiation (ΔR).

indicating already observed and reported significant energy dependent response [9,10] of the GafChromic™ XR-QA2® film model.

2.4. CTDI measurements using film strips

Both Head and Body CTDI phantoms containing film strips were irradiated via single axial mode scan with corresponding beam qualities listed in Table 2. Range of mAs used was from 300 to 600 mAs and collimator opening was set to be 20 mm. For the Head CTDI phantom axial scan we used the head bow-tie filter and for the scan performed on Body CTDI phantom the body bow-tie filter was used.

Reflectance change of film strips irradiated within CTDI phantom was converted into air kerma in air using previously established calibration curves (given in Fig. 3). Since the film strips were irradiated within the CTDI phantom, measured signal incorporates scattering component and is assumed to represent air kerma in phantom [15], which was subsequently converted into absorbed dose to water following the AAPM TG-61 document [13].

In a first approximation, the assumption is that the beam quality within CTDI phantom does not change significantly when compared to the beam quality in the air. Therefore, in order to obtain dose to water at measurement points, reflectance change line profile through the film strip is first converted to air kerma in phantom and then multiplied by the mass-energy absorption coefficient ratio water to air $(\mu_{en}/\rho)^{wat}_{air}$ for the given beam quality in the air (Fig. 4):

$$D_{HVL-air}(x) = \left(\frac{\mu_{en}}{\rho}\right)^{wat}_{air}\Bigg|_{HVL-air} (K_{air})^{phantom}_{HVL-air}(\Delta R) \quad (1)$$

where $(K_{air})^{phantom}_{HVL-air}(\Delta R)$ represents air kerma in phantom determined

Table 2
Beam qualities used in this work to perform CTDI measurements.

Beam kVp [keV]	Filtration	HVL_{air} [mm Al]
100	Head	5.3
	Body	6.3
120	Head	6.2
	Body	7.3
140	Head	7.2
	Body	8.2

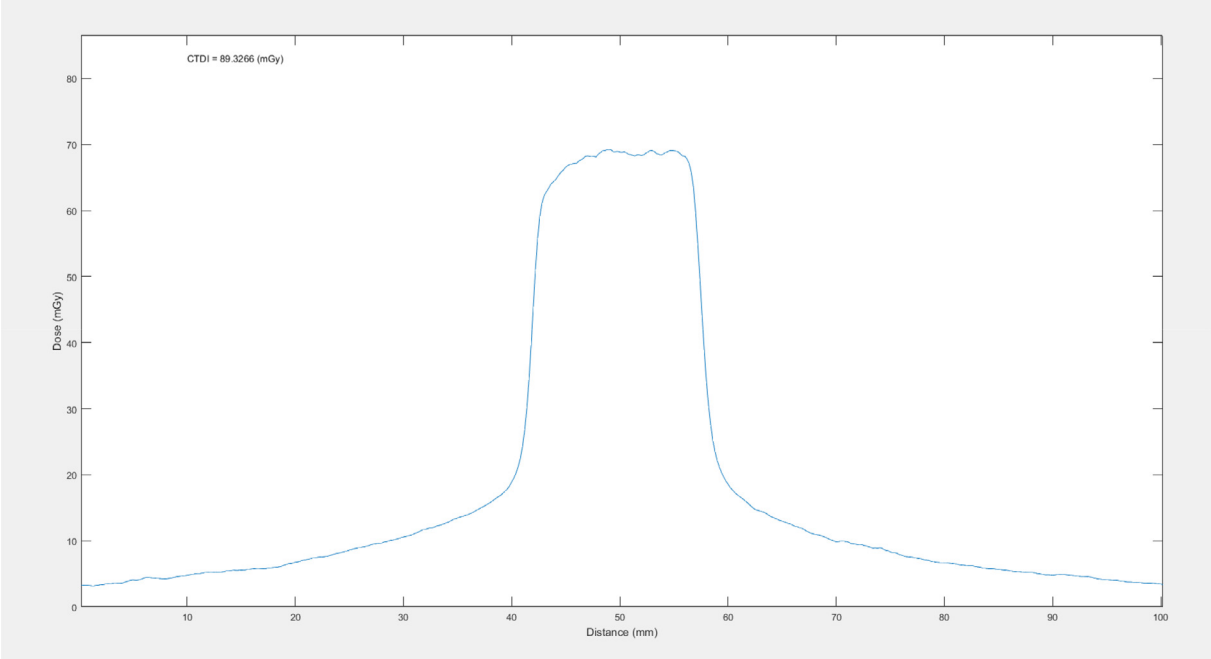

Fig. 4. Dose profile measurement obtained using radiochromic film strip in one of the peripheral positions within Body CTDI phantom.

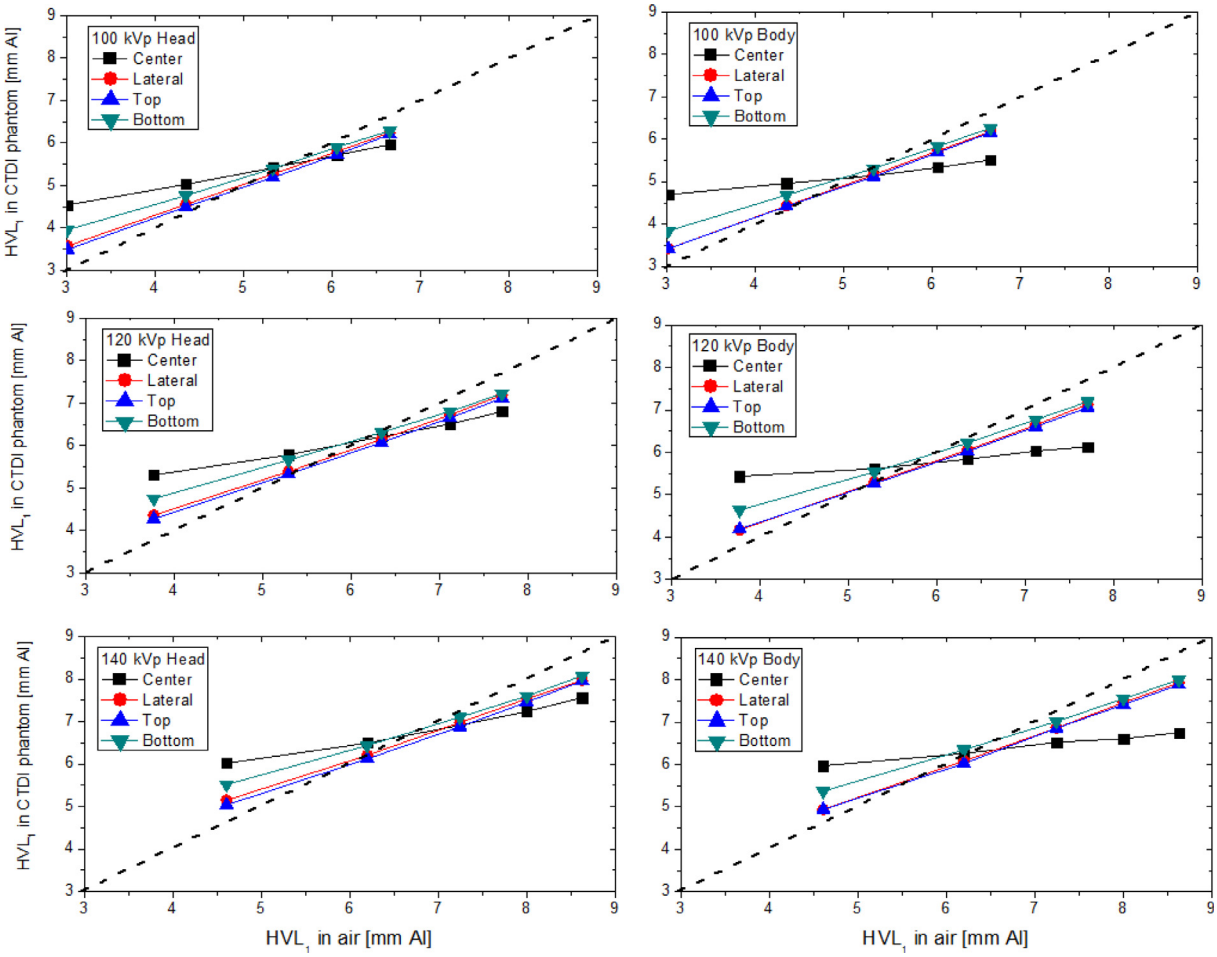

Fig. 5. Monte Carlo simulations of photon spectra changes within Head and Body CTDI phantom for various beam qualities in the air entering the CTDI phantom.

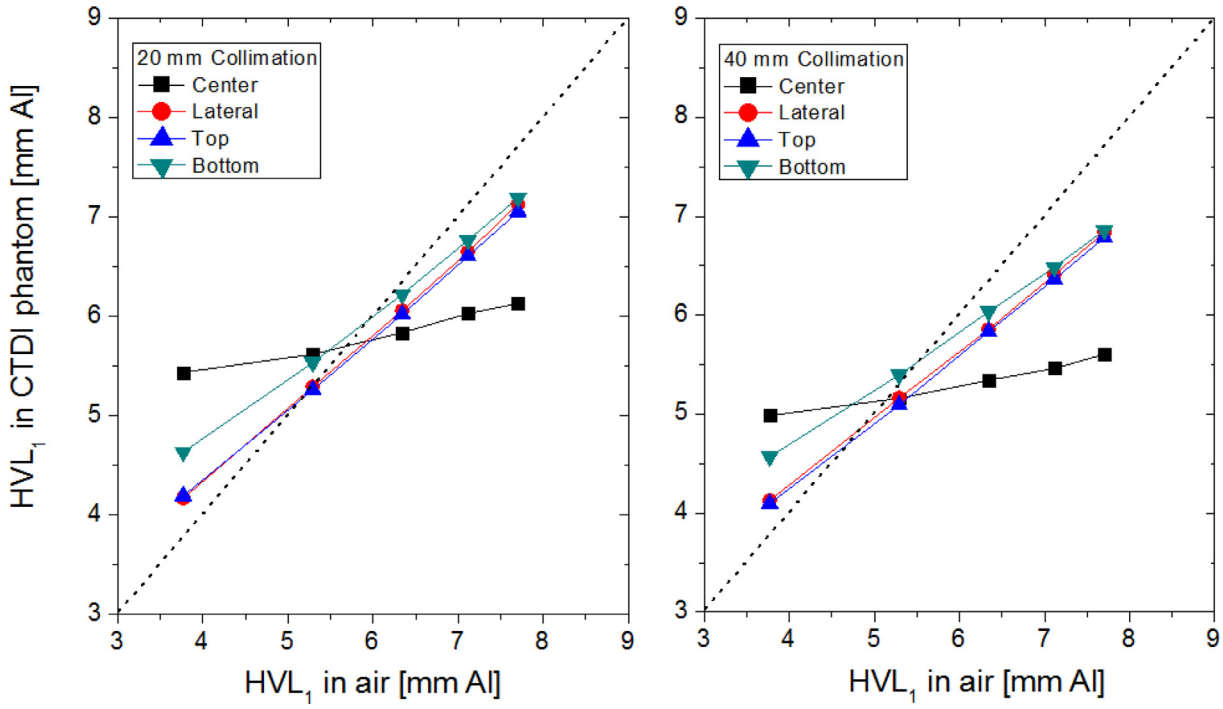

Fig. 6. Monte Carlo simulations of HVL changes within Head CTDI phantom as a function of beam quality in air for the fan beam geometry with 20 mm (left) and 40 mm (right) collimation.

for beam quality specified by HVL-air for the measured response (ΔR).

From the dose profile given in Fig. 4, the measured $CTDI_{100}$ is calculated as an integral value over the 100 mm length at the center of the film piece (1):

$$CTDI_{100}^{HVL-air} = \frac{1}{NT}\int_{-50mm}^{+50mm} D_{HVL-air}(x) \quad (2)$$

with NT being 20 mm in our case.

The same procedure is repeated for all five measuring positions within the CTDI phantom, and the weighted CTDI is calculated as:

$$CTDI_{w}^{HVL-air} = \frac{1}{6}[CTDI_{100}^{HVL-air}(@3) + CTDI_{100}^{HVL-air}(@6) + CTDI_{100}^{HVL-air}(@9) + CTDI_{100}^{HVL-air}(@12)] + \frac{1}{3}CTDI_{100}^{HVL-air}(@center) \quad (3)$$

The CTDI measurement methodology given by Eqs. (1–3) assumes that beam quality does not change significantly within CTDI phantom from the beam quality in air. However, if the beam quality is known at each measurement point (within each of the five CTDI phantom holes) the appropriate calibration curve as well as the mass energy-absorption coefficient ratio water to air $(\mu_{en}/\rho)_{air}^{wat}$ could have been used for dose profile determination:

$$D_{HVL-phantom}(x) = \left(\frac{\mu_{en}}{\rho}\right)_{air}^{wat}\Bigg|_{HVL-phantom} (k_{air})_{HVL-phantom}^{phantom}(\Delta R) \quad (4)$$

where HVL-phantom corresponds to the beam quality at the top, bottom, left, right or center positions within the CTDI phantom, and $(k_{air})_{HVL-phantom}^{phantom}(\Delta R)$ represents air kerma in phantom obtained for the appropriate beam quality (HVL-phantom). So, in pursuing the beam quality correction method, Eq. (4) replaces Eq. (1) above, while the Eqs. (2) and (3) remain the same.

We have performed measurements of $CTDI_w$ in both Head and Body CTDI phantoms for six beam qualities listed in Table 2. Having a range of beam quality changes for various imaging beams within CTDI phantom, obtained from MC simulations, we calculated $CTDI_w$ using Eq. (3) and its corresponding corrected value $CTDI_w^{cor}$ using Eq. (4) and compared them.

3. Results and discussion

Fig. 5 summarizes results of MC simulations of photon spectra changes obtained for various beam qualities in the air for two Head and Body CTDI phantoms. Photon spectra were sampled in each of the file holes within CTDI phantoms and corresponding HVLs were calculated and plotted as a function of the HVL in the air for the beam quality impinging on the phantoms. Due to cylindrical symmetry, left (9′clock) and right (3′clock) positions within the CTDI phantoms were represented as a single point labeled lateral. Dashed lines in Fig. 5 indicate the approximation in which the HVL in the air was used to calculate dose profiles within CTDI phantom.

Our results suggest that for all kVp settings and both phantom sizes low penetrating beams (with low HVL values) will exhibit a beam hardening effect. On the other hand, more penetrating beams (with high HVL values) will soften within CTDI phantom. The beam hardening effect for low HVL beams can be explained by the predominant presence of photo-effect interactions of the primary photon beam, which primarily removes low energy photons. On the other hand, the beam softening of high HVL beams is governed by the presence of mainly scattered photons having lower energy than the energy of the incoming beam. Also, the simulated HVL values within CTDI phantom cluster together and cross the dashed lines (Fig. 5), indicating that for certain beam qualities the approximation of using the same HVL for each of the five measurement holes within CTDI phantom as the one in the air is valid. The crossing point between HVLs in phantom and in the air is increasing with the increase of kVp. Monte Carlo simulations show that the largest change in the HVL values occurs at the central position of the CTDI phantom.

Results presented in Fig. 5 have been obtained from Monte Carlo simulations with fan beam geometry defined by 20 mm collimation that is mostly used with head CT scanning protocols, On the other hand, Fig. 6 represents HVL changes within CTDI phantom as a function of HVL beam quality in the air for two collimation settings, i.e., 20 mm

Table 3
Measured CTDIw values obtained without and with the correction for the beam quality change within CTDI phantom and the difference between them for six different beam qualities.

Beam kVp [keV]	Filtration	HVL_{air} [mm Al]	$CTDI_w$ [mGy]	Corrected $CTDI_w$ [mGy]	% Difference
100	Head	5.3	30.5	30.6	+0.30
	Body	6.3	36.7	35.8	−2.45
120	Head	6.2	47.5	47.0	−1.05
	Body	7.3	56.1	53.2	−5.17
140	Head	7.2	65.6	64.2	−2.13
	Body	8.2	75.7	71.4	−5.68

(left) and 40 mm (right), both calculated for 120 kVp setting. As expected, the beam hardening effect (dominated by photo-effect) is less affected for larger (40 mm) fan beam collimation. For 20 mm collimation, the change in HVL at 3.8 mm Al beam quality in the air is 42% while for the 40 mm collimation it amounts to 34%. On the other hand, for the higher HVL values where the photon scattering becomes dominant, the beam softening effect is more pronounced for larger (40 mm) collimation. For 20 mm collimation, the change in HVL at 7.7 mm Al beam quality in the air is 26% while for the 40 mm collimation it amounts to 37%.

The obtained percentage difference between corrected and uncorrected $CTDI_w$ values for six different beam qualities is given in Table 3. Observed differences are in the range from +0.30% to –2.13% for CTDI measurements within Head CTDI phantom, and from −2.45% to −5.68% for CTDI measurements within Body CTDI phantom. Results presented in Table 3 can be explained by the observed changes in HVLs (presented in Fig. 5), indicating that scattering (being more pronounced in larger size Body CTDI phantom) is the dominant effect governing the correction in the proposed method of CTDI measurements using reference radiochromic film dosimetry system. On the other hand, results in Table 3 also suggest that difference becomes larger for higher beam qualities. This indicates that not only the scattering but the beam penetration too plays a role in beam quality change throughout the CTDI phantom during the CT scanning geometry in which X-ray beam takes a full rotation around the phantom.

4. Conclusions

In this work, we performed Monte Carlo simulations of photon spectra within both Head and Body CTDI phantoms for a number of beam qualities used in diagnostic CT scanners, with HVLs ranging from 3 to 8.6 mm Al. We found that for beam qualities having low HVL in the air, the photon spectra harden within the CTDI phantom. On the other hand, for beam qualities with high HVL in the air values, the photon spectra soften within the CTDI phantom. We also demonstrated the XR-QA2 GafChromic™ film model based reference dosimetry system that can provide CTDI values with the appropriate calibration curve and the ratio of mass energy-absorption coefficient $(\mu_{en}/\rho)^{wat}_{air}$ for the given beam quality at a given measurement point within the CTDI phantom.. For the most commonly used beam quality in CT-imaging (120 kVp) and for our CT scanner we observed a difference between in-phantom beam quality change corrected CTDIw and uncorrected CTDIw to be 1% for the Head filter within Head CTDI phantom and 5.7% for the Body filter within Body CTDI phantom.

Acknowledgements

This work was supported in part by the Natural Sciences and Engineering Research Council of Canada contract No. 386009. We would like to thank Dr Ernesto Mainegra-Hing and Dr Peter Watson for their assistance in Monte Carlo simulations and HVL calculations.

References

[1] McCollough C, Cody D, Edyvean S, Geise R, Gould B, The Keat N, et al. Reporting, and management of radiation dose in CT. Report of AAPM Task Group 23. CT Dosimetry 2008.
[2] Shope TB, Gagne RM, Johnson GC. A method for describing the doses delivered by transmission x-ray computed tomography. Med Phys 1981;8:488–95.
[3] Dixon RL, Anderson JA, Donovan BM, Boedeker K, Boone JM, Cody DD. Comprehensive methodology for the evaluation of radiation dose in X-ray computed tomography. Report of AAPM Task Group 111. Future CT Dosimetry 2010.
[4] DeWerd LA, Wagner LK. Characteristics of radiation detectors for diagnostic radiology. Appl Radiat Isot 1999;50:125–36.
[5] Angelone M, Chiti M, Esposito A, Fantuzzi E, Monteventi F. Energy dependence of TLD-300 response from 6 keV up to 1250 keV. Radiat Prot Dosimetry 2002;100:381–4.
[6] Reft CS. The energy dependence and dose response of a commercial optically stimulated luminescent detector for kilovoltage photon, megavoltage photon, and electron, proton, and carbon beams. Med Phys 2009;36:1690–9.
[7] Rampado O, Gareli E, Ropolo R. Computed tomography dose measurements with radiochromic films and a flatbed scanner. Med Phys 2010;37:189–96.
[8] Quintero C, Tomic N, Bekerat H, DeBlois F, Seuntjens J, Devic S. CTDI Measurements using a Radiochromic Film-based clinical protocol. Med Phys 2014;41:10.
[9] Tomic N, Quintero C, Whiting BR, Aldelaijan S, Bekerat H, Liang L, et al. Characterization of the calibration curves and energy dependence GafchromicTM XR-QA2 model based radiochromic film dosimetry system. Med Phys 2014;41. https://doi.org/10.1118/1.4876295. 062105.
[10] Lillo F, Mettivier G, Sarno A, Tromba G, Tomic N, Devic S, et al. Energy dependent calibration of XR-QA2 radiochromic film with monochromatic and polychromatic x-rays beams. Med Phys 2016;43:583–8. https://doi.org/10.1118/1.4939063.
[11] Zhang D, DeMarco J, Cagnon C, Turner A, Khatonabadi M, McNitt-Gray M. Change in X-Ray Ct spectra inside of dosimetry phantoms: beam hardening or beam softening. Med Phys 2011;38:3844. https://doi.org/10.1118/1.3613473.
[12] Poludniowski G, Landry G, DeBlois F, Evans PM, Verhaegen F. SpekCalc: a program to calculate photon spectra from tungsten anode x-ray tubes. Phys Med Biol. 2009;54:N433–8.
[13] Ma CM, Coffey CW, DeWerd LA, Liu C, Nath R, Seltzer SM, et al. AAPM protocol for 40–300 kV x-ray beam dosimetry in radiotherapy and radiobiology. Med Phys 2001;28:868–93.
[14] Devic S, Tomic N, Lewis D. Reference radiochromic film dosimetry: review of technical aspects. Phys Med 2016;32:541–56.
[15] Tomic N, Devic S, DeBlois F, Seuntjens J. Reference radiochromic film dosimetry in kilo-voltage photon beams during CBCT image acquisition. Med Phys 2010;37:1083–92.